FACTA UNIVERSITATIS
Series: **Electronics and Energetics** Vol. 31, N° 2, June 2018, pp. 313 - 328
https://doi.org/10.2298/FUEE1802313M

THE SURFACE RECOMBINATION VELOCITY AND BULK LIFETIME INFLUENCES ON PHOTOGENERATED EXCESS CARRIER DENSITY AND TEMPERATURE DISTRIBUTIONS IN N-TYPE SILICON EXCITED BY A FREQUENCY-MODULATED LIGHT SOURCE

Dragana K. Markushev[1], Dragan D. Markushev[2], Slobodanka Galović[3], Sanja Aleksić[1], Dragan S. Pantić[1], Dragan M. Todorović[4]

[1]Faculty of Electronic Engineering, University of Niš, Niš, Serbia
[2]Institute of Physics, University of Belgrade, Belgrade-Zemun, Serbia
[3]Vinča Institute of Nuclear Sciences, Belgrade, Serbia
[4]Institute for Multidisciplinary Research, University of Belgrade, Belgrade, Serbia

Abstract. *The temperature distributions in the n-type silicon circular plate, excited by a frequency-modulated light source from one side, are investigated theoretically in the frequency domain. The influence of the photogenerated excess carrier density on the temperature distributions is considered with respect to the sample thickness, surface quality and carrier lifetime. The presence of the thermalization and non-radiative recombination processes are taken into account. The existence of the fast and slow heat sources in the sample is recognized. It is shown that the temperature distribution on sample surfaces is a sensitive function of an excess carrier density under a bulk and surface recombination. The most favorable values of surface velocities ratio and bulk lifetime are established, assigned for a simpler and more effective analysis of the carrier influence in semiconductors. The photothermal and photoacoustic transmission detection configuration is proposed as a most suitable experimental scheme for the investigation of the excess carrier influence on the silicon surface temperatures.*

Key words: *semiconductor, surface recombination, bulk lifetime, photogeneration, excess carriers, periodic thermal excitation, temperature distribution, frequency domain, photothermal, photoacoustic.*

Received August 23, 2017; received in revised form November 9, 2017
Corresponding author: Sanja Aleksić
Faculty of Electronic Engineering, University of Niš, 14 Aleksandra Medvedeva, 18000 Niš, Serbia
(E-mail: sanja.aleksic@elfak.ni.ac.rs)

1. INTRODUCTION

It is a well known fact that the basis of photoacoustic (PA) and photothermal techniques (PT) is a photo-induced change in the thermal state of the sample. When a modulated light is used to excite a sample, part of the light energy is absorbed and used to periodically increase its internal energy resulting in a sample heating. A periodic sample heating causes a periodic temperature change in a sample, both on its surfaces and in the bulk [1-3].

The evolution of solid-state materials and the development of the technology for integrated circuit and/or microelectromechanical systems (MEMS) fabrication bring silicon (Si) as well as other crystalline semiconductor materials in focus of modern PT investigations [4-9]. Our ability to understand the influence of the thermal propagation and carrier transport processes on the thermal state of Si and other semiconductors is based on a detailed understanding of the solid-state physics in retrospect, as well as on the development of the new theoretical and experimental PA and PT methods and models necessary to turn the "pure" theory into the "measurable" reality [10-13].

A variety of PA and PT methods can be used to characterize the semiconductors in details [14-17]. The temperature changes can be detected measuring directly a sample surface temperature variations or perturbations of temperature-dependent thermodynamic parameters, such as pressure or density. These parameters changes are detected with various transducers, assuming that the transducer signal intensity is proportional to the amplitude of the measured parameter and depends of temperature propagation across the investigated sample and its environment [18-20]. There are several different experimental schemes that can be used to efficiently detect temperature changes in irradiated semiconductor samples having the form of circular or rectangular plates. One of the most simple and popular among them is the so-called PA transmission detection configuration [20-22]. Such scheme assumes that the sample "front" surface is irradiated by the modulated optical beam, and the transducer detects the signal behind the "rear" one.

The thermal state of the illuminated semiconductor depends, beside the others, on the density of photogenerated excess carriers and their generation and recombination ratios in response to the light-matter interaction. The reason for that lies in the fact that the generation of periodic excess carriers in semiconductors will produce thermal waves induced by the carrier thermalization and recombination processes. These processes are responsible for the existence of fast and slow thermal sources within the semiconductor. A fast thermal source exists due to the thermalization of carriers to the band gap. Slow thermal sources exist due to the recombination of carriers in the bulk and on the surface of the sample. Slows are directly dependent on the density of the photogenerated carriers [23-25].

The lifetime of the photogenerated excess carriers is a single value parameter usually referring to the carrier recombination lifetime in the material bulk [26,27]. This bulk lifetime is dependent on the carrier density and doped atoms concentrations. Carriers move from regions where their density is high to regions where their density is low during their lifetime. This transport mechanism, called the carrier diffusion, is associated with a random motion of carriers. Such motion is characterized with the carrier diffusion length, the average length a carrier covers between generation and recombination. The carrier diffusion length is related to the bulk lifetime and carrier diffusivity [29]. Knowing that, the diffusion length can be used as a convenient parameter to define the relative thickness of the semiconductor sample.

Besides the bulk, the semiconductor surface also plays an important role in recombination. A recombination on the surfaces is typically described by a surface lifetime. It depends,

besides other things, on the sample thickness and surface recombination velocities on the front and rear surfaces of the sample [30]. Higher values of recombination velocities means a large number of recombination centers (active states) created by the abrupt termination of the semiconductor crystal. The reduction of these centers using some conventional chemical or mechanical methods is known as a surface passivation. One can expect the decrease of the recombination velocity during the passivation.

The surface and bulk generation and recombination effects on photogenerated carrier densities and temperature distributions can be analyzed by various PA and PT measuring techniques [3,8,24,31]. In the case of PA methods, when the photoinduced effects are measured and analyzed as the function of the optical source modulated frequency, the sample response depends practically only on the periodically variable temperature (i.e. the distribution of periodically variable photogenerated carriers). The steady temperature and carrier density components does not have the effect on the photoacoustic response. This is the reason why, in all theoretical considerations, only periodic (quasi-static) components is taken into account [32-35]. On the other hand, transients can be ignored in the analysis of signals as the function of a periodic optical excitation [22,31].

The object of this paper is to investigate theoretically the influence of photogenerated excess carrier densities on temperature distribution in n-type silicon circular plate irradiated from one side, both on sample surfaces and in the bulk. The assumptions with respect to the surface and bulk lifetime changes are taken into account as parameters closely connected to the various PA and PT measurement conditions and configurations. Detailed thermal source analysis is presented as a function of modulation frequency in the range of (10^1-10^7) Hz and sample thickness higher (thick sample) and lower (thin sample) then the excess carrier diffusion length.

2. THEORETICAL BACKGROUND

Photogenerated carrier dynamics

Doped semiconductors contain majority and minority carriers. In the case of n-type silicon, majority carriers are electrons and minority carriers are holes. Excess carriers (electrons and holes) can be generated in semiconductors illuminating them with modulated light source. A necessary condition is that the energy of the light photon is larger than the band gap of the material. Both minority and majority carriers are generated when a photon is absorbed. The number of majority carriers in an irradiated semiconductor does not alter significantly. The opposite is true for the number of minority carriers. The number of photogenerated minority excess carriers outweighs the number of minority carriers existing in the doped sample. Therefore, the number of minority carriers in an irradiated sample can be approximated by the number of light generated excess carriers.

If we assume that the excess carrier transport happens due to diffusion only, and accept a simple model that defines recombination-generation rates proportional to the minority excess carrier density, we can write time-dependent 1D diffusion equation for holes along the *x*-axes in the low-level donor density n-type silicon [5,22]:

$$\frac{\partial \delta n_p(x,t)}{\partial t} = D_p \frac{\partial^2 \delta n_p(x,t)}{\partial x^2} + G_p(x,t) - R_p(x,t), \tag{1}$$

where $\delta n_p(x,t)$ is the excess minority carriers – holes density, D_p is the hole diffusivity, $G_p(x,t)$ is the volumetric rate of the holes generation and $R_p(x,t)$ is the volumetric rate of

the holes recombination. Simple equations can be used to define $G_p(x,t)$ and $R_p(x,t)$ assuming modulated light excitation [5,6]:

$$G_p(x,t) = \frac{\beta I_0}{\varepsilon} e^{-\beta x} \frac{1}{2}(1+e^{i\,\omega t}) \text{ and } R_p(x,t) = \frac{\delta n_p(x,t)}{\tau} = \frac{\delta n_p(x)}{\tau}\frac{1}{2}(1+e^{i\omega t}), \quad (2)$$

where I_0 is the incident light intensity, ε is the photon energy, β is the semiconductor material absorption coefficient, $\omega = 2\pi f$, f is the light modulation frequency, $\tau = \tau_p$ is the holes bulk lifetime and $\delta n_p(x)$ is the spatial part of $\delta n_p(x,t)$.

If the general solution of Eq. (1) is given by $\delta n_p(x,t) = (1/2)\ \delta n_p(x)\cdot(1 + e^{i\omega t})$, one can obtain steady (Eq.(3.a)) and periodic (Eq.(3.b)) components of the equation explaining the excess carriers (holes) dynamics in the sample [22,23,31]:

$$\frac{\mathrm{d}^2\delta n_p(x)}{\mathrm{d}x^2} - \frac{\delta n_p(x)}{L_p^2} = -\frac{\beta I_0}{\varepsilon D_p} e^{-\beta x}, \quad (3.a)$$

$$\frac{\mathrm{d}^2\delta n_p(x,\omega)}{\mathrm{d}x^2} - \frac{\delta n_p(x,\omega)}{L_\omega^2} = -\frac{\beta I_0}{\varepsilon D_p} e^{-\beta x}, \quad (3.b)$$

where $L_\omega = L_p \big/ \sqrt{(1+i\omega\tau)}$, $L_p = \sqrt{D_p \tau}$ is the holes diffusion length, and $\delta n_p(x,\omega)$ is the periodic excess carrier density. For the sake of simplicity, we will denote $\delta n_p(x,\omega) = \delta\mu_p(x)$ in all further analysis. Assuming that only $\delta\mu_p(x)$ is responsible for sample response (PA case), the general solution of Eq. (3.b) can be written in the form:

$$\delta\mu_p(x) = [A_{1\omega}e^{x/L} + A_{2\omega}e^{-x/L}] \; - \; \frac{\beta I_0}{\varepsilon D_p(\beta^2 - L_\omega^{-2})} e^{-\beta x}, \quad (4)$$

where $A_{1\omega}$ and $A_{2\omega}$ are the integration constants, which can be obtained using proper boundary conditions. Boundary conditions, among other things, introduce the surface recombination velocities s onto the front (s_1) and back (s_2) sample surface, as the parameters used to define surface recombination process efficiency: a higher value of s means a higher recombination efficiency. In our case, boundary conditions are given by:

$$D_p \left.\frac{\mathrm{d}\delta\mu_p(x)}{\mathrm{d}x}\right|_{x=0} = s_1 \cdot \delta\mu_p(0) \text{ and } D_p \left.\frac{\mathrm{d}\delta\mu_p(x)}{\mathrm{d}x}\right|_{x=l} = -s_2 \cdot \delta\mu_p(l), \quad (5)$$

where the sample front surface is at $x = 0$, and rear is at $x = l$.

Using Eqs.(3-5), the constants $A_{1\omega}$ and $A_{2\omega}$ can be calculated and presented in the following form:

$$A_{1\omega} = \frac{A_\omega}{a}\cdot[(v_{D\omega} - s_2)(v_\beta + s_1)e^{-l/L} - (v_{D\omega} + s_1)(v_\beta - s_2)e^{-\beta l}], \quad (6a)$$

$$A_{2\omega} = \frac{A_\omega}{a}\cdot[(v_{D\omega} + s_2)(v_\beta + s_1)e^{l/L} - (v_{D\omega} - s_1)(v_\beta - s_2)e^{-\beta l}], \quad (6b)$$

$$A_\omega = \frac{\beta I_0}{\varepsilon D_p(\beta^2 - L_\omega^{-2})}, \quad (6c)$$

and

$$a = [v_{D\omega} + s_1]\cdot[v_{D\omega} + s_2]e^{l/L} - [v_{D\omega} - s_1]\cdot[v_{D\omega} - s_2]e^{-l/L}. \quad (6d)$$

Here $v_{D\omega} = D_p / L_\omega$ and $v_\beta = \beta D_p$ are excess carrier's diffusion velocities.

Temperature distribution with excess carrier influence

The excess carrier generation, recombination and transport processes affect the spatial temperature distribution $T_s(x,t) = T_{st}(x) + \mathrm{Re}(\theta_s(x)e^{i\omega t})$ within the sample, where $T_{st}(x)$ is the steady and $\mathrm{Re}(\theta_s(s)e^{i\omega t})$ is the periodic (quasi-static) component (modulated light source is assumed). Taking into account PA simplification, only $\mathrm{Re}(\theta_s(x)e^{i\omega t})$ component will be considered in our further analysis [32,33]. To include the excess carrier influence $\delta\mu_p(x)$ is used (Eq.(4)) within the $\theta_s(x)$ calculations. Assuming that thermalization $H_{\mathrm{therm}}(x)$, bulk $H_{\mathrm{br}}(x)$ and surface $H_{\mathrm{sr}}(x)$ recombination heat sources exists in the sample, the 1D thermal diffusion equation can be written in the form [22,23,31]:

$$\frac{\mathrm{d}^2\theta_s(x)}{\mathrm{d}x^2} - \sigma_\omega^2\theta_s(x) = -\frac{1}{k}[H_{\mathrm{therm}}(x) + H_{\mathrm{br}}(x)], \quad (7)$$

where $\sigma_\omega = (1+i)\sqrt{\pi f / D}$ is the complex heat diffusion coefficient, $D = k/(\rho c)$ is the thermal diffusivity of the sample (k – is the heat conductivity, ρ – is the density, c – is the heat capacity) and:

$$H_{\mathrm{therm}}(x) = \frac{\varepsilon - \varepsilon_g}{\varepsilon}\beta I_0 \exp(-\beta x), \quad (8.a)$$

$$H_{\mathrm{br}}(x) = -\frac{\varepsilon_g}{\tau}\delta\mu_p(x), \quad (8.b)$$

where ε_g is the semiconductor band gap energy. The surface recombination heat sources $H_{\mathrm{sr}}(0)$ and $H_{\mathrm{sr}}(l)$ are incorporated in boundary conditions on the front ($x = 0$) and back ($x = l$) sample surfaces:

$$-k\left.\frac{\mathrm{d}\theta_s(x)}{\mathrm{d}x}\right|_{x=0} = s_1\delta\mu_p(0)\cdot\varepsilon_g \text{ and } -k\left.\frac{\mathrm{d}\theta_s(x)}{\mathrm{d}x}\right|_{z=l} = -s_2\delta\mu_p(l)\cdot\varepsilon_g \quad (9)$$

General solution of the Eq. (7), using boundary conditions (Eq. (9)), can be written as a total temperature distribution $\theta_s(x)$ given by a vector sum of the thermalization $\theta_{\mathrm{therm}}(x)$, bulk $\theta_{\mathrm{br}}(x)$ and surface $\theta_{\mathrm{sr}}(x)$ recombination components as a result of three different heat generation mechanisms [21,22,31]:

$$\theta_s(x) = \theta_{\mathrm{therm}}(x) + \theta_{\mathrm{br}}(x) + \theta_{\mathrm{sr}}(x), \quad (10)$$

where

$$\theta_{\mathrm{therm}}(x) = \frac{I_0}{k}\frac{\varepsilon - \varepsilon_g}{\varepsilon}\frac{\beta}{\beta^2 - \sigma_\omega^2}\left[b\frac{e^{\sigma_\omega(x-l)} + e^{-\sigma_\omega(x-l)} - e^{-\beta l}(e^{\sigma_\omega x} + e^{-\sigma_\omega x})}{e^{\sigma_\omega l} - e^{-\sigma_\omega l}} - e^{-\beta x}\right], \quad (11.a)$$

$$\theta_{\mathrm{br}}(x) = \frac{\varepsilon_g B_1}{\tau k\sigma_\omega^2}\left\{\frac{B_2 e^{\sigma_\omega x} + B_3 e^{-\sigma_\omega x}}{e^{\sigma_\omega l} - e^{-\sigma_\omega l}} - \frac{1}{c^2 - 1}\left[\frac{\delta\mu_p(x)}{B_1} + \frac{b^2 - c^2}{b^2 - 1}e^{-\beta x}\right]\right\}, \quad (11.b)$$

$$\theta_{sr}(x) = \frac{2\varepsilon_g}{k\sigma_\omega} \frac{s_1 \delta\mu_p(0)\cosh[\sigma_\omega(x-l)] + s_2 \delta\mu_p(l)\cosh(\sigma_\omega x)}{e^{\sigma_\omega l} - e^{-\sigma_\omega l}}, \tag{11.c}$$

with

$$b = \frac{\beta}{\sigma_\omega}, \; c = \frac{1}{L_\omega \sigma_\omega},$$
$$B_1 = -A_\omega,$$
$$B_2 = B_4 e^{-\sigma_\omega l} + B_5,$$
$$B_3 = B_4 e^{\sigma_\omega l} + B_5,$$

and

$$B_4 = -c \frac{\frac{1}{B_1}[\delta\mu_p(l) - \delta\mu_p(0)\cosh(l/L_\omega)] - \cosh(l/L_\omega) + e^{-\beta l}}{\sinh(l/L_\omega)\cdot(c^2-1)} - \frac{b}{b^2-1},$$

$$B_5 = c \frac{\frac{1}{B_1}[\delta\mu_p(l)\cosh(l/L_\omega) - \delta\mu_p(0)] - 1 + e^{-\beta l}\cosh(l/L_\omega)}{\sinh(l/L_\omega)\cdot(c^2-1)} + \frac{be^{-\beta l}}{b^2-1}.$$

3. RESULTS AND DISCUSSIONS

Our simulations were performed assuming the photogenerated carriers 1D transport along the *x*-axes (sample thickness). The illuminated sample front surface is at $x = 0$ and its rear surface is at $x = l$. The samples were supposed to be n-type Si circular plates with the donor density $N_D = 2\times10^{15}$ cm^{-3}. The resistivity ρ_{Si} and hole diffusivity D_p are found to be: $\rho_{Si} = 2{,}37\ \Omega\cdot$cm and $D_p = 12$ cm^2/s [5]. Carrier (holes) bulk lifetime is taken to be $\tau = 10^{-4}$ s [4,5,27]. It is assumed that the sample is excited by a 5 mW red laser diode light ($\lambda = 660$ nm) modulated in the frequency f range of (10–10^7) Hz. Upper frequency limit is defined by the condition $2\pi f\tau_{therm} \le 1$ [32-35] where $\tau_{therm} \to 10^{-8}$ s is the assumed Si thermal relaxation time [35-36]. This condition allows the similar behavior of the $\theta_s(x)$ spectra predicted by the Fourier parabolic or Cattaneo–Vernotte hyperbolic theoretical models. Lower frequency limit is determined by the fact that in the case of $f \ge 10$ Hz we are able to separate the influence of individual $\theta_s(x)$ components. Within the given frequency range it is assumed that the temperatures of all quasi-particle subsystems are the same [33].

A simple ratio between the sample thickness l and holes diffusion length L_p appears in many equations written above, affecting the behavior of the carrier density and temperature distribution in the frequency domain. The presented analysis was performed assuming the existence of two groups of samples defined by a relative thickness: thick in the case of $l / L_p > 1$; thin in the case of $l / L_p < 1$. In both cases, for given τ, $L_p = 346.4$ μm. Each group is characterized with specific effects within the carrier density or temperature distributions induced by photogenerated carriers. The 1000 μm thick silicon plate was taken as a typical representative of the thick samples. The 10 μm thick plate represents the thin ones.

Our calculations were performed regarding the silicon surface quality changing the values of recombination velocities in the front and in the rear. Bulk lifetime changes are

taken into account, too. They are closely connected to the sample material quality due to defects and impurities.

Finally, our analysis is focused on the front and rear sample surfaces, characterized with the different levels of carrier influence on $\theta_s(x)$. This type of analysis could help one to find the best method and experimental conditions within the PA and PT measurements to obtain the significant influence of photogenerated carriers on semiconductor thermal response.

Carrier density: Surface recombination influence

In order to simplify the analysis and to understand better the photogenerated excess carrier density behavior in the frequency domain, $\delta\mu_p(x)$ amplitudes A are considered rather than phases. To calculate A Equation (1) is used with different values of recombination speeds s_1 and s_2, and constant holes bulk lifetime ($\tau = 10^{-4}$ s). The values of s are taken to be 0 m/s and 24 m/s representing totally passive and active surface respectively [20,22,23,31]. The value of τ corresponds to the assumed N_D value [5,6,27]. It must be noted here that in reality most silicon wafers have higher levels of contaminants and thus shorter lifetimes than used here. Calculated density amplitudes on the front $\delta\mu_p(0)$ and rear $\delta\mu_p(l)$ sample surface as a function of modulation frequency f are shown in Figure 1.

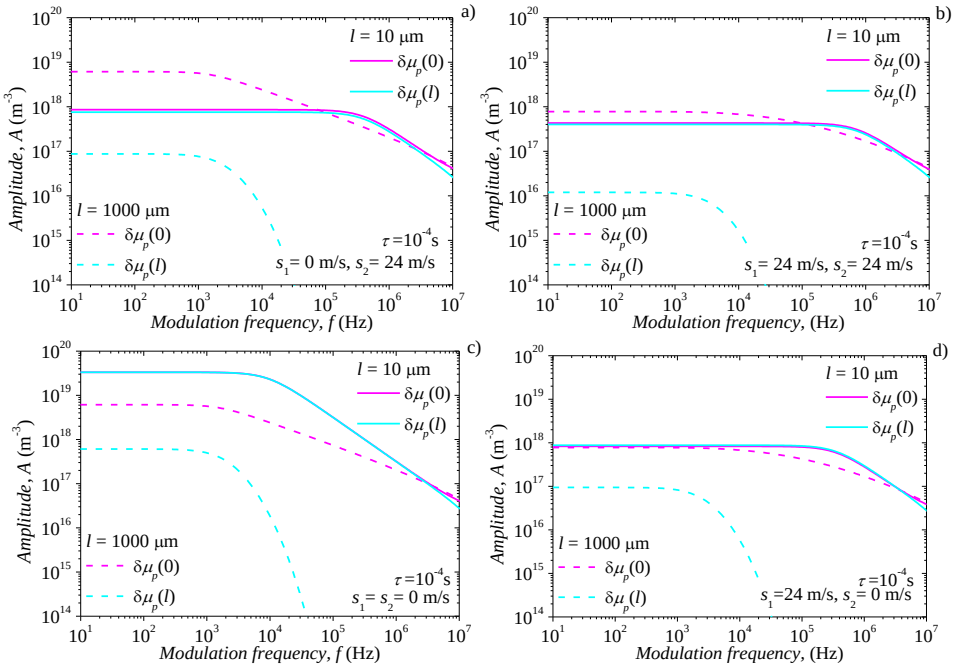

Fig. 1 Comparison of the excess carrier density $\delta\mu_p(x)$ amplitudes A at front ($\delta\mu_p(0)$ – magenta) and rear ($\delta\mu_p(l)$ - light blue) surface versus modulation frequency f, in the case of a thick (l = 1000 μm – dash) and thin (l = 10 μm – solid) sample. Different surface recombination velocities s_1 and s_2 ratios are presented (a,b,c,d) assuming constant lifetime value $\tau = 10^{-4}$ s.

In the case of thick samples, results show that there is an enormously greater density of excess carriers on the front surface, while rear density is at least one order of magnitude lower. A brief numerical analysis shows that $\delta\mu_p(0) \sim L_\omega$ and $\delta\mu_p(l) \sim L_\omega \cdot e^{-l/L_\omega}$. Both densities are independent of frequency when $\omega\tau << 1$. At higher frequencies, a sharp decrease of $\delta\mu_p(0)$ and $\delta\mu_p(l)$ is expected with different slopes. Obviously, $\delta\mu_p(l)$ is much more sensitive to the sample thickness l than $\delta\mu_p(0)$ is.

In the case of thin samples, results show that both $\delta\mu_p(0)$ and $\delta\mu_p(l)$ values are almost identical. At lower frequencies, they are independent of frequency approaching the limit density values for the given s_1 and s_2 ratio. At higher frequencies, l/L_ω ratio determines their behavior. In the case of $l/L_\omega < 1$, a sharp decrease of both densities is expected with the same slope. In the case of $l/L_\omega \geq 1$, a sharp decrease of $\delta\mu_p(l)$ continues but $\delta\mu_p(0)$ slope becomes smaller.

An exception must be made in the case of a full passivation on both surfaces ($s_1 = s_2 = 0$) presented in Figure 1.c. The obtained values of $\delta\mu_p(0)$ and $\delta\mu_p(l)$ at lower frequencies are much higher than those calculated for other s_1 and s_2 ratios. At higher frequencies, the densities on both surfaces start to decrease following L_ω frequency dependence till $l/L_\omega \geq 1$, when they start to differ ($f \approx 10^7$ Hz).

It is a well known fact that the correct understanding of the carrier density influence on the thermal state of the sample sometimes lies in the analysis of a density change, not of its absolute value [3,31]. Knowing that, the amplitude ratio A_r of the carrier density on the front and back of the sample ($A_r = |\delta\mu_p(0)/\delta\mu_p(l)|$) was taken as a suitable parameter for our analysis. The results of such analysis in frequency domain as a function of the sample thickness and different s_1 and s_2 ratios are shown in Figure 2. As follows from this Figure, the highest values of density ratios (red lines) are obtained when the illuminated front sample surface is perfectly passivated ($s_1 = 0$ m/s) while the rear one has a high recombination ($s_2 = 24$ m/s). This result will be used in further analysis as the most suitable recombination velocities ratio in which the effects of the excess carriers are most obvious.

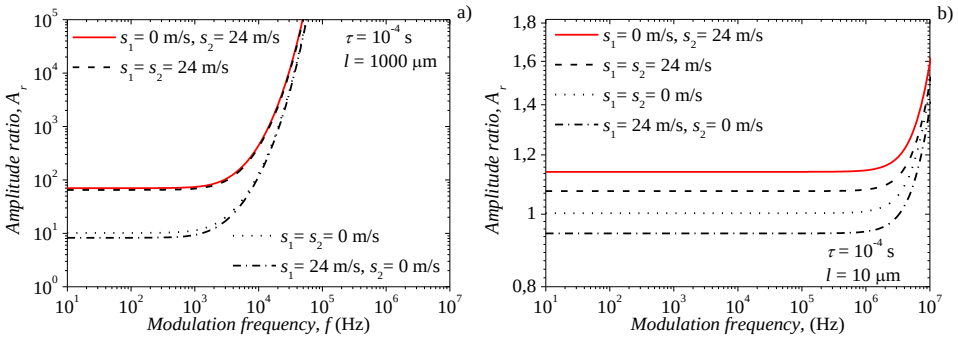

Fig. 2 Comparison of the photogenerated excess carrier density amplitude ratio $A_r = |\delta n_p(0)/\delta n_p(l)|$ between front and rear surface versus modulation frequency f, calculated for different surface recombination velocities s_1 and s_2 ratios and constant $\tau = 10^{-4}$ s in the case of: a) thick (l = 1000 μm) and b) thin (l = 10 μm) sample.

Carrier density: Bulk lifetime influence

The Equation (1) is used again to calculate the photogenerated excess carrier density $\delta\mu_p(x)$ amplitude A with different values of bulk lifetimes and constant values of s_1 = 0 m/s and s_2 = 24 m/s. The values of τ are taken to be between 10^{-4} s and 5×10^{-7} s representing low- and high-level donor density values N_D respectively. A shorter lifetime also means a higher level of Si crystal lattice defects and/or contaminants. Calculated densities on the front $\delta\mu_p(0)$ and rear $\delta\mu_p(l)$ sample surface as a function of the modulation frequency f are shown in Figure 3.

In the case of thick samples, the results show that, besides an enormously greater density of excess carriers on the front surface, the rear density sharply decreases by decreasing the bulk lifetime, reaching the limit of 1 carrier per unit volume at $\tau = 5 \times 10^{-7}$ s. As mentioned before, both densities are independent of frequency when $\omega\tau << 1$. It is seen that $\delta\mu_p(0)$ and $\delta\mu_p(l)$ decrease at higher frequencies with different slopes. As follows from this analysis, $\delta\mu_p(l)$ is much more sensitive to lifetime changes than $\delta\mu_p(0)$ is.

In the case of thin samples, the results again show that $\delta\mu_p(0)$ and $\delta\mu_p(l)$ shapes in the frequency domain are almost identical, having a weak dependence on the lifetime changes. Calculated for the same s_1 and s_2 ratio, both density values remain constant at lower frequencies, decreasing at higher ones following l / L_ω ratio. No significant differences between $\delta\mu_p(0)$ and $\delta\mu_p(l)$ are found except at very high frequencies ($l / L_\omega \geq 1$).

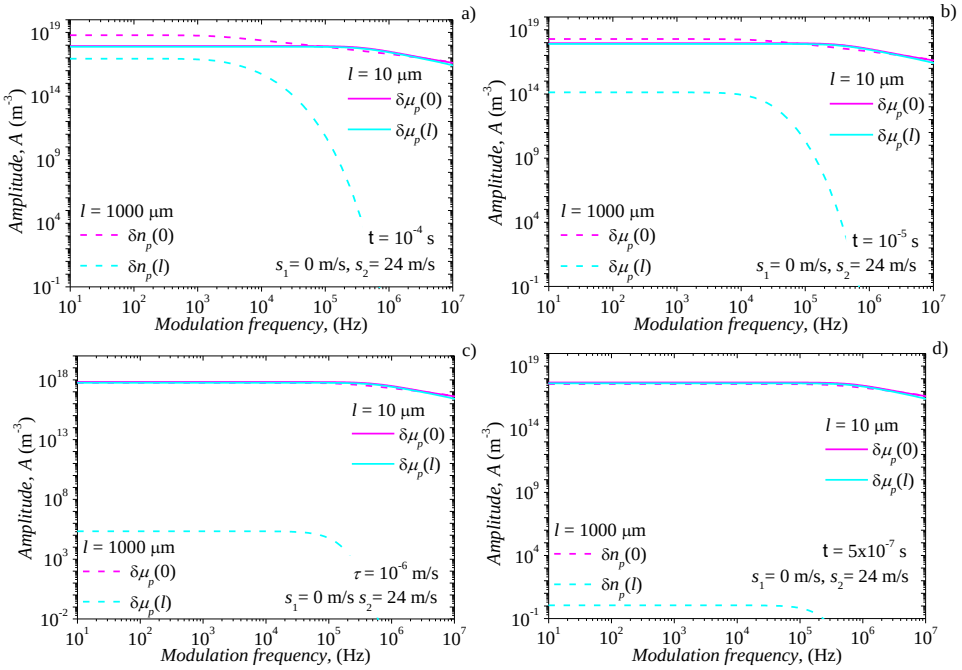

Fig. 3 Comparison of the excess carrier density $\delta\mu_p(x)$ amplitudes A at front ($\delta\mu_p(0)$ – magenta) and rear ($\delta\mu_p(l)$ – light blue) surface versus modulation frequency f, in the case of a thick (l = 1000 μm – dash) and thin (l = 10 μm – solid) sample. Different lifetime τ values are taking into account (a,b,c,d) assuming constant s_1 and s_2 ratio.

In order to further survey the influence of the photogenerated excess carriers, we performed the analysis of amplitude ratios *Ar* ($A_r = |\delta\mu_p(0)/\delta\mu_p(l)|$) in the case of thick and thin samples presented in Figure 3. The results of such an analysis in frequency domain are shown in Figure 4. It is clear that the less intensive ratios are assigned to the higher τ values. In our calculation, higher values of the lifetime means lower levels of defects and contaminants in the sample. This fact allows for a simpler analysis of carrier transport effects in the sample. Therefore, in our further calculations, the value of $\tau = 10^{-4}$ s (red lines) will be taken as the basis for the study of excess carrier effect on the thermal properties of a semiconductor.

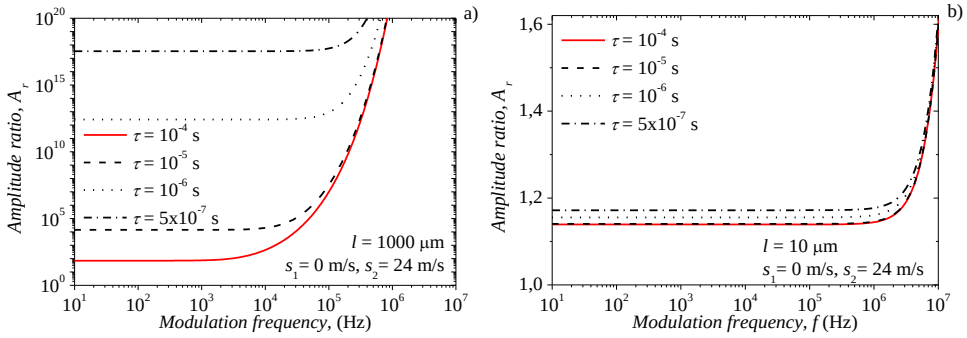

Fig. 4 Comparison of the excess carrier density amplitude ratio A_r between front and rear surface $|\delta n_p(0)/\delta n_p(l)|$ versus modulation frequency *f*, calculated for different values of bulk lifetimes τ and constant s_1 and s_2 ratio in the case of: a) thick (l = 1000 μm) and b) thin (l = 10 μm) sample.

Total surface temperature: Excess carrier contributions

Based on the results obtained in previous sections and the established most convenient parameter values (s_1 = 0 m/s, s_2 = 24 m/s, $\tau = 10^{-4}$ s) assigned for the study of the excess carrier influence, the dependences of the total temperature distributions $\theta_s(x)$ and its components ($\theta_{therm}(x)$, $\theta_{br}(x)$ and $\theta_{sr}(x)$) on the modulation frequency *f* are presented in Figures 5 and 6. Their normalized amplitudes A_n and phases φ are calculated using Eqs. (10) and (11) on the front ($x = 0$) and rear ($x = l$) sample surfaces in the case of thick (l = 1000 μm) and thin (l = 10 μm) samples. The amplitude normalization is performed using the same values of light intensity I_0 to make different temperature distribution components comparable to each other. All calculations are performed assuming that the absorption of the incident light in the surrounding media is negligible.

In the case of thick samples, the results show that on the front surface (Figure 5.a,b) and at lower frequencies ($f < 10^3$ Hz), the photogenerated excess carrier contribution to the $\theta_s(x)$ is significant through the bulk recombination component $\theta_{br}(x)$. At higher frequencies ($f > 10^3$ Hz), the $\theta_{therm}(x)$ component predominates, so no significant excess carrier contribution to the $\theta_s(x)$ can be found. $\theta_{sr}(x)$ component is negligible in the whole frequency range, which is expected (s_1 = 0 m/s). On the rear surface (Figure 5.c,d), the excess carrier contribution to the $\theta_s(x)$ can be found in the whole frequency range: at lower frequencies the $\theta_{br}(x)$ contributes significantly; at higher frequencies $\theta_{sr}(x)$ predominates (s_2 = 24 m/s).

This $\theta_s(x)$ analysis confirm previously obtained results [22,23,31] and must hold for all sample thicknesses satisfying the condition $l / L_p > 1$.

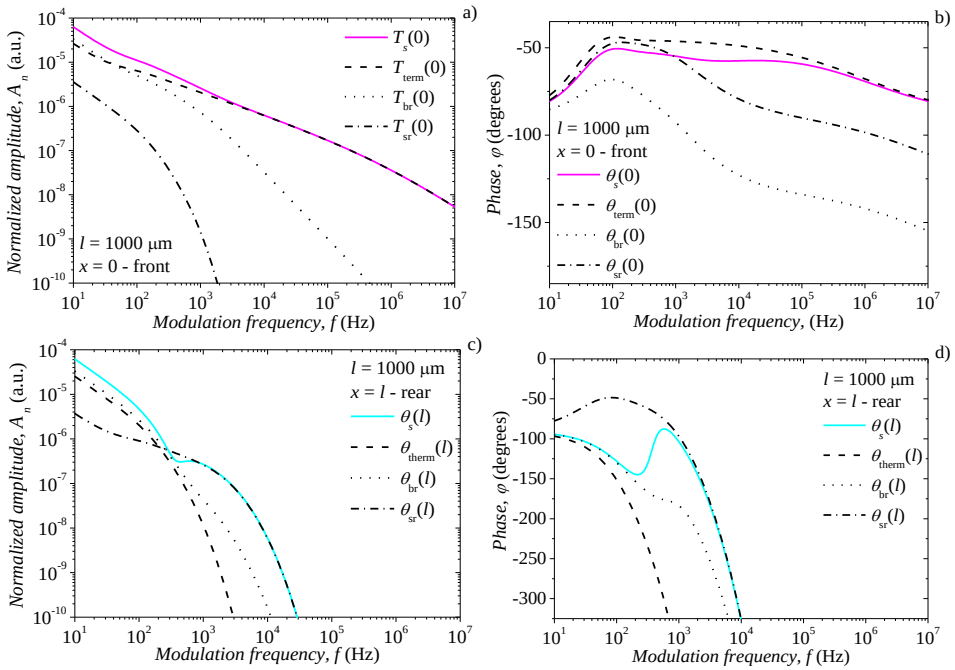

Fig. 5 Comparison of the surface temperature distribution $\theta_s(x)$ normalized amplitude A_n and phase φ at front (a,b – solid magenta) and rear surface (c,d – solid light blue) of a thick sample (l = 1000 μm), with thermalization ($\theta_{therm}(x)$ – dash), bulk recombination ($\theta_{bulk}(x)$ – dot) and surface recombination ($\theta_{sr}(x)$ – dash-dot) contributions versus modulation frequency f.

In the case of thin samples, the results show that on the front surface (Figure 6.a,b), the photogenerated excess carrier contribution to the $\theta_s(x)$ is significant in almost whole frequency range through the surface recombination component $\theta_{sr}(x)$. Only at very high frequencies ($f > 10^5$ Hz) $\theta_{therm}(x)$ component dominates, so no significant excess carrier contribution to the $\theta_s(x)$ can be found. $\theta_{br}(x)$ component is negligible in the whole frequency range, which is expected ($l << L_p$). On the rear surface (Figure 5.c,d), the excess carrier contribution to the $\theta_s(x)$ can be found in the whole frequency range, where $\theta_{sr}(x)$ component dominates. As far as we know, especially in the case of higher frequencies, this kind of $\theta_s(x)$ analysis was not presented in any article published before. It must hold for all sample thicknesses satisfying the condition $l / L_p < 1$, indicating that in the case of thin samples and higher frequencies $\theta_s(0)$ at front illuminated surface could drop much faster than $\theta_s(l)$ at rear non-illuminated one. Such $\theta_s(x)$ behavior may result in a major change of PA and PT signals, especially for those taking into account temperatures from both surfaces (e.g. PA thermoelastic signals) [22,23,31].

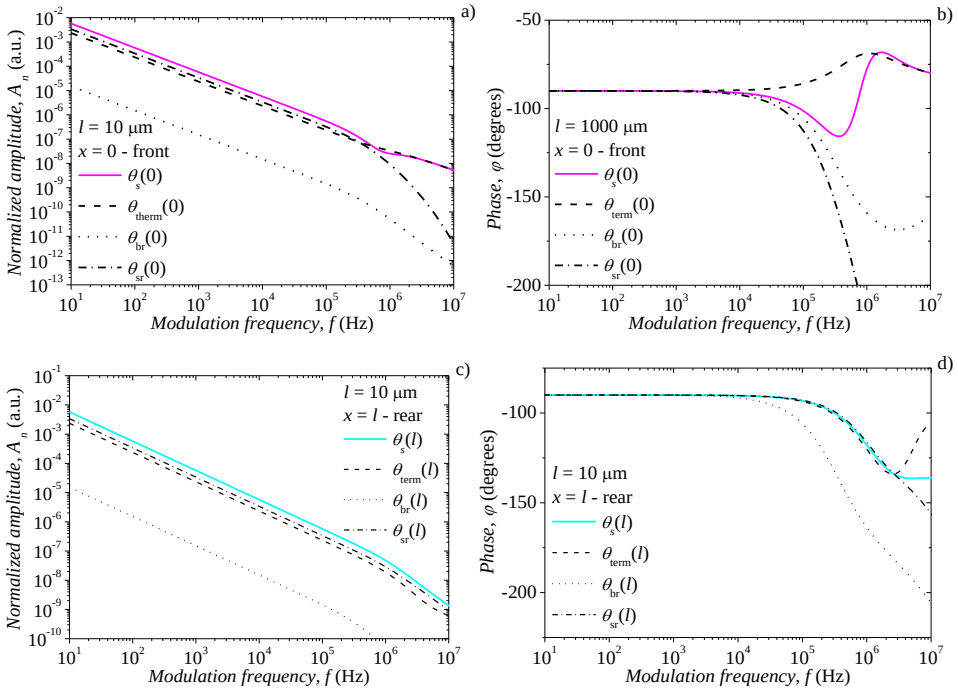

Fig. 6 Comparison of the surface temperature distribution $\theta_s(x)$ normalized amplitude A_n and phase φ at front (a,b – solid magenta) and rear surface (c,d – solid light blue) of a thin sample (l = 10 μm), with thermalization ($\theta_{therm}(x)$ – dash), bulk recombination ($\theta_{bulk}(x)$ – dot) and surface recombination ($\theta_{sr}(x)$ – dash-dot) contributions versus modulation frequency f.

Based on the results presented in Figures 5 and 6, we analyze amplitude ratios A_r and phase differences $\Delta\varphi$ between $\theta_s(x)$ and $\theta_i(x)$, where i = therm, br and sr. The results of such an analysis are presented in Figures 7 (tick) and 8 (thin samples). Obviously, the back surface of the thick and thin samples suffers the greatest influence of photogenerated carriers. Therefore, we can recommend the transmission detection configuration as the most favorable experimental PA or PT scheme for studying the influence of free carriers on the thermal state on silicon surfaces.

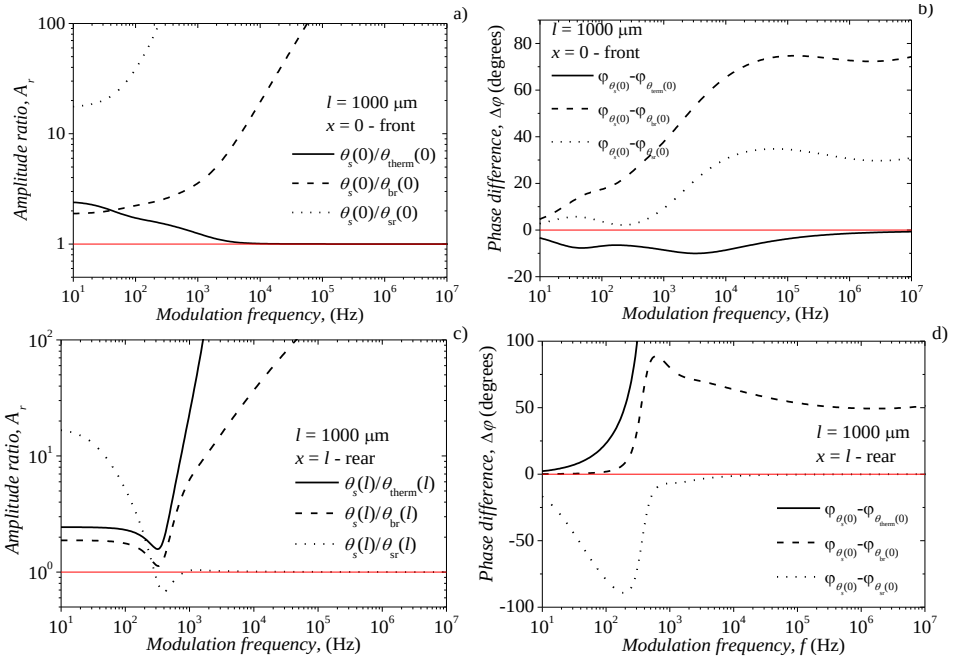

Fig. 7 Comparison of the amplitude ratios A_r and phase differences $\Delta\varphi$ at front (a,b) and rear surface (c,d) of a thick sample (l = 1000 μm) versus modulation frequency f.

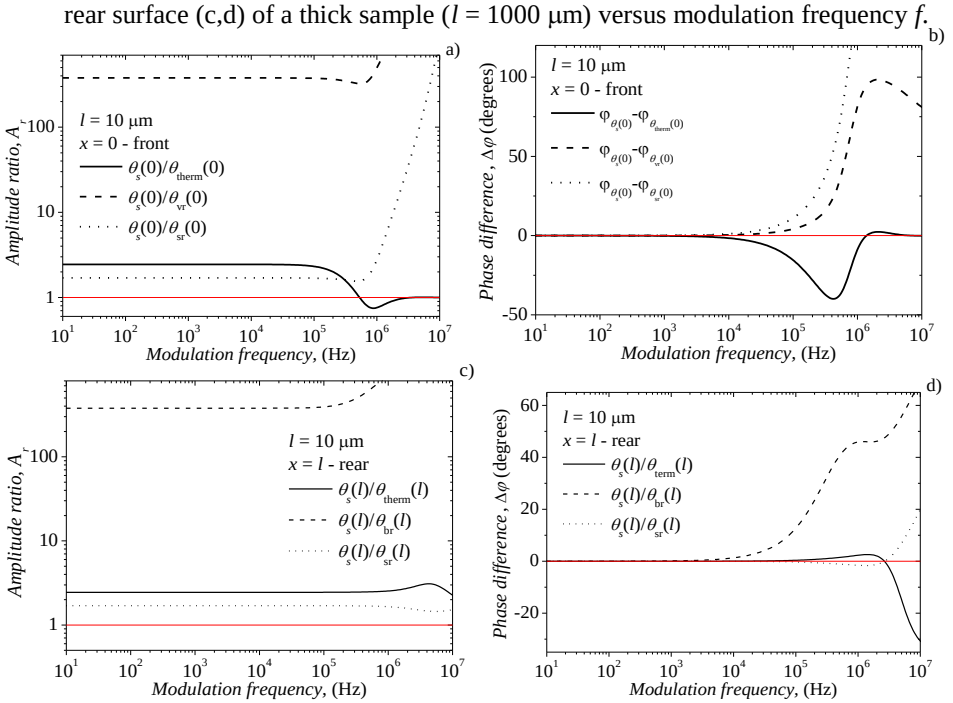

Fig. 8 Comparison of the amplitude ratios ratios A_r and phase differences $\Delta\varphi$ at front (a,b) and rear surface (c,d) of a thin sample (l = 10 μm) versus modulation frequency f.

4. CONCLUSIONS

By the combination of the photogenerated excess carrier density and heat source analysis in n-type silicon excited by a frequency-modulated light source, we established the most favorable values of surface velocities and bulk lifetime assigned for the examination of the excess carrier influence on temperature distributions at the semiconductor surfaces. These analyses were performed by a theoretical study of the carrier density and temperature amplitudes and phases in the case of thin (10 μm) and thick (1000 μm) silicon circular plates as a function of modulation frequencies in the range of $(10 - 10^7)$Hz. The relative thickness of the samples is defined by the ratio of sample thickness l and carrier diffusion length L_p: $l/L_p > 1$ thick and $l/L_p < 1$ thin.

It was demonstrated that the photogenerated excess carrier density strongly depends on the sample surface characteristics and material quality described by the surface recombination velocity and bulk lifetime respectively. We suggest that the most intensive excess carrier influence in thick and thin samples could be found when the illuminated front surface is perfectly passivated ($s_1 = 0$ m/s) and the rear has a high recombination ($s_2 = 24$ m/s). Also, we propose a high value for the carriers bulk lifetime ($\tau = 10^{-4}$s), which implies a low concentration of dopant and internal defects, allowing a much simpler analysis of the carrier transport in semiconductors.

Furthermore, a detailed heat source analysis was performed to demonstrate the effects of photogenerated carriers on the surface temperature distributions. In the case of thick samples, this analysis predicts a strong influence of the bulk recombination on both surfaces and at lower frequencies ($f < 10^3$ Hz). At higher frequencies ($f > 10^3$ Hz), a strong surface recombination influence can be found only on the rear surface. In the case of thin samples, the bulk recombination is negligible but the surface recombination dominates: on the rear surface at all frequencies; on the front surface at $f < 10^5$ Hz. Also, on the front surface of thin samples one can expect sudden decrease of the total temperature at higher frequencies due to the changed roles of temperature components (thermalization and surface recombination).

This kind of analysis allows one to choose which type of the experimental set-up, transmission or reflection is much convenient to use due to a free carrier influence study. The results of our study predict a strong influence of the recombination processes on the rear sample surfaces in the whole range of frequencies regardless of the thickness. Therefore, the transmission photoacoustic or photothermal configuration can be recommended as the most suitable experimental scheme for studying the influence of photogenerated carriers on surface temperatures.

Acknowledgements: *This work has been supported by the Ministry of Education, Science and Technological Development of the Republic of Serbia under the grant ON171016.*

REFERENCES

[1] L. A. Skvortsov, "Laser photothermal spectroscopy of light-induced absorption", *Quantum Electronics*, vol. 43, pp. 1–13, 2013.
[2] P. Almond, P. Patel, 1996 *Photothermal Science and Technique* (London: Chapman and Hall)
[3] S. Bialkowski, 1996 *Photothermal Spectroscopy Methods for Chemical Analysis* (New York: John Wiley)
[4] B. G. Streetman and S. Banerjee, 2000 *Solid State Electronic Devices*, 5th edition (Prentice Hall)
[5] S. M, Sze, Semiconductor Devices Physics and Technology, 2nd edition, (1985, 2002) by John Wiley & Sons

[6] Shyn Wang, Fundamentals of Semiconductor Theory and Device Physics, Prentice Hall International, Inc, Englewood Cliiffs, Nj 07632, USA, ISBN 0-13-344425-2)
[7] Y. Chen, Y. Dai, H. Chou, I. Chang, " Photoinduced Absorption Studied by Photothermal Deflection Spectroscopy: Its Application to the Determination of the Energy of Dangling-Bond States in a-Si:H", *Chinese Journal of Physics*, vol. 31, pp. 767-772, 1993.
[8] J. Kitao, Y. Kasuya, T. Kunii, N. Yoshida, S. Nonomura, "Photoinduced effects on infrared and near infrared absorption of amorphous and microcrystalline Si measured by photothermal bending spectroscopy", *Analytical Sciences*, vol. 17, pp. 302-304, 2001.
[9] M.A. Nigro, M. Gagliardi, F.G.D. Corte, "Measurement of the IR absorption induced by visible radiation in amorphous silicon and silicon carbide thin films by an in-guide technique", *Optical Materials*, vol. 30, p. 1240, 2008.
[10] L. Goris, K. Haenen, M. Nesládek, P. Wagner, D. Vanderzande, L. Schepper, J. D'haen, L. Lutsen, J. Manca, "Absorption phenomena in organic thin films for solar cell applications investigated by photothermal deflection spectroscopy", *Journal of Materials Sciences*, vol. 40, pp. 1413-1418, 2005.
[11] K. Tanaka, T. Gotoh, N. Yoshida, S. Nonomura, "Photothermal deflection spectroscopy of chalcogenide glasses", *Journal of Applied Physics*, vol. 91, p. 125, 2002.
[12] L. Xiao, L. Changyoung, L. Zhang, Y. Zhao, S. Jia, G. Zhou, "Pulsed-laser Pumped Photothermal Deflection Spectroscopy for Liquid Thermal Diffusivity Measurement", *Chinese Journal Lasers B*, vol. B9, pp. 538-544, 2000.
[13] Li Y., Gupta R., "An investigation of the photothermal deflection spectroscopy technique for temperature measurements in a flame" *Applied Physics B: Lasers and Optics*, 75, 103-112 (2002)
[14] Photoacoustic and Thermal Wave Phenomena in Semiconductors by A. Mandelis (Editor), 1987 (North-Holland)
[15] J. Batista, A. Mandelis and D. Shaughnessy, "Temperature dependence of carrier mobility in Si wafers measured by infrared photocarrier radiometry", *Appl. Phys. Lett.*, vol. 82, pp. 4077-4079 (Jun. 9, 2003).
[16] K.M. Gupta, Nishu Gupta, "Carrier Transport in Semiconductors" in Advanced Semiconducting Materials and Devices, Part of the series Engineering Materials (2016) (Springer International Publishing Switzerland), pp 87-144.
[17] Igor Lashkevych, Oleg Titov and Yuri G Gurevich, Recombination and temperature distribution in semiconductors, *Semiconductor Science and Technology*, vol. 27, 055014 (7pp), 2012.
[18] Arnau Vives A. 2008 *Piezoelectric Transducers and Applications* (Springer-Verlag Berlin Haidelberg New York),
[19] Min-hang Bao 2000 *Micro Mechanical Transducers: Pressure Sensors, Accelerometers, and Gyroscopes Handbook of Sensors and Actuators, Volume 8,* (Elsevier Publishing Company)
[20] D.D. Markushev, M.D. Rabasovic, D.M. Todorovic, S. Galovic, S.E. Bialkowski, *Review of Scientific Instruments*, vol. 86, p. 035110, 2015.
[21] Schroder, Dieter K. *Semiconductor Material and Device Characterization* 2006, 3rd Ed. John Wiley and Sons, Inc. Hoboken, New Jersey.
[22] D. M. Todorović, P. M. Nikolić, M. D. Dramićanin, D. G. Vasiljević, Z. D. Ristovski, "Photoacoustic frequency heat-transmission technique: Thermal and carrier transport parameters measurements in silicon", *Journal of Applied Physics*, vol. 78, p. 5790, 1995.
[23] D. M. Todorović, P. M. Nikolić, A. I. Bojičić, and K. T. Radulović, " Thermoelastic and electronic strain contributions to the frequency transmission photoacoustic effect in semiconductors" *Physical Review B*, vol. 55, pp. 15631–15642, 1997.
[24] A. Mandelis, R. Bleiss, F. Shimura, "Highly resolved separation of carrier- and thermal-wave contributions to photothermal signals from Cr-doped silicon using rate-window infrared radiometry", *Journal of Applied Physics*, vol. 74, p. 3431, 1993 .
[25] Y. G Gurevich, I. Lashkevych, "Sources of Fluxes of Energy, Heat, and Diffusion Heat in a Bipolar Semiconductor: Influence of Nonequilibrium Charge Carriers", *International Journal of Thermophysics*, vol. 34, p. 341, 2013.
[26] O. Palais, J. Gervais, S. Martinuzzi, "High resolution lifetime scan maps of silicon wafers", *Materials Science and Engineering: B*, vol. 71, pp. 47-50, 2000.
[27] Andres Cuevas, Daniel Macdonald, "Measuring and interpreting the lifetime of silicon wafers", *Solar Energy*, vol. 76, no. 1-3, pp. 255-262, 2003.
[28] K.T. Radulović, P.M. Nikolić, D. Vasiljević-Radović, D. M. Todorović, S.S. Vujović, A.I. Bojicić, V. Blagojević, D. Urosević, "A Contribition of Carrier Transport Processes to the Photoacoustic Effects in Doped Narrow Gap Semiconductors", *Review of Scientific Instruments*, vol. 74, p. 595, 2003.

[29] Gary Hodes, Prashant V. Kamat, "Understanding the Implication of Carrier Diffusion Length in Photovoltaic Cells", *The Journal of Physical Chemistry Letters*, vol. 6, pp. 4090−4092, 2015**.**

[30] A. B. Sproul, "Dimensionless solution of the equation describing the effect of surface recombination on carrier decay in semiconductors", *Journal of Applied Physics*, vol. 76, pp. 2851-2854, 1994.

[31] M. D. Dramićanin, P. M. Nikolić, Z. D. Ristovski, D. G. Vasiljević, and D. M. Todorović, "Photoacoustic investigation of transport in semiconductors: Theoretical and experimental study of a Ge single crystal", *Physical Review B*, vol. 51, pp. 14226, 1995.

[32] Yuri G. Gurevich, Georgiy N.Logvinov, Gerardo G. de la Cruz, and Gabino Espejo Lopez, "Physics of thermal waves in homogeneous and inhomogeneous (two-layer) samples", *International Jornal of Thermal Sciences*, vol. 42, pp. 63-69, 2003.

[33] G. Gonzalez da la Cruz and Yu. G. Gurevich, Thermal diffusivity of a two-layered systems, *Physical Review B*, vol. 51, pp. 2188-2192, 1995.

[34] Ordonez-Miranda, J.J. Alvarado-Gil, "Determination of thermal properties for hyperbolic heat transport using a frequency-modulated excitation source", *International Journal of Engineering Science*, vol. 50, pp. 101–112, 2012.

[35] S. Galovic and D. Kostoski, "Photothermal wave propagation in media with thermal memory", *Journal of Applied Physics*, vol. 93, pp. 3063-3070, 2003.

[36] A. Vedavarz, S. Kumar, & M. K. Moallemi, "Significance of non-Fourier heat waves in conduction", *Journal of Heat Transfer–Transactions of the ASME*, vol. 116, pp. 221–224, 1994.